Molecular Pharmacology Fast Forward. Published on July 25, 2011 as doi: 10.1124/mol.111.072751

MOL Manuscript # 72751

TITLE PAGE

Inhibition of Navβ4 peptide-mediated resurgent sodium currents in Nav1.7 channels by carbamazepine, riluzole and anandamide

Jonathan W. Theile and Theodore R. Cummins

Department of Pharmacology and Toxicology, Stark Neurosciences Research Institute, Indiana University School of Medicine, Indianapolis, IN 46202, USA

Department of Pharmacology and Toxicology, Stark Neurosciences Research Institute (JWT, TRC)

Molecular Pharmacology Fast Forward. Published on July 25, 2011 as DOI: 10.1124/mol.111.072751
This article has not been copyedited and formatted. The final version may differ from this version.

RUNNING TITLE PAGE

a) Running title: Inhibition of Nav1.7 resurgent currents

b) Correspondence:

Jonathan Theile

Department of Pharmacology and Toxicology

Stark Neurosciences Research Institute

Indiana University School of Medicine

950 West Walnut Street, R2-459

Indianapolis, IN 46202, USA

317-278-9343

317-278-5849 (fax)

E-mail: jontheile@yahoo.com

c) Manuscript counts:

Text pages: 27 (Abstract thru references)

Figures: 7

Tables: 2

References: 39

Abstract: 249

Introduction: 728

Discussion: 1,243

d) Abbreviations

AEA, anandamide; CBZ, carbamazepine; DMSO, dimethyl sulfoxide; DRG, dorsal root ganglion; IEM, inherited erythromelalgia; I_{NaR}, resurgent current; I/V, current-voltage; PEPD, paroxysmal extreme pain disorder; RZ: riluzole

Molecular Pharmacology Fast Forward. Published on July 25, 2011 as DOI: 10.1124/mol.111.072751
This article has not been copyedited and formatted. The final version may differ from this version.

Abstract

Paroxysmal extreme pain disorder (PEPD) and inherited erythromelalgia (IEM) are inherited pain syndromes arising from different sets of gain-of-function mutations in the sensory neuronal sodium channel isoform, Nav1.7. Mutations associated with PEPD, but not IEM, result in destabilized inactivation of Nav1.7 and enhanced resurgent sodium currents. Resurgent currents arise following relief of ultra-fast open-channel block mediated by an endogenous blocking particle and are thought to influence neuronal excitability. As such, enhancement of resurgent currents may constitute a pathological mechanism contributing to sensory neuron hyperexcitability and pain hypersensitivity associated with PEPD. Furthermore, pain associated with PEPD, but not IEM, is alleviated by the sodium channel inhibitor carbamazepine. We speculated that selective attenuation of PEPD-enhanced resurgent currents might contribute to this therapeutic effect. Here we examined whether carbamazepine and two other sodium channel inhibitors, riluzole and anandamide, exhibit differential inhibition of resurgent currents. To gain further insight into the potential mechanism(s) of resurgent currents, we examined whether these inhibitors produced correlative changes in other properties of sodium channel inactivation. Using stably transfected HEK293 cells expressing wild-type Nav1.7 and the PEPD mutants, T1464I and M1627K, we examined the effects of the three drugs on Navβ4-peptide mediated resurgent currents. We observed a correlation between resurgent current inhibition and a drug-mediated increase in the rate of inactivation and inhibition of persistent sodium currents. Furthermore, although carbamazepine did not selectively target resurgent currents, anandamide strongly inhibited resurgent currents with minimal effects on the peak transient current amplitude, demonstrating that resurgent currents can be selectively targeted.

Molecular Pharmacology Fast Forward. Published on July 25, 2011 as DOI: 10.1124/mol.111.072751
This article has not been copyedited and formatted. The final version may differ from this version.

Introduction

Voltage gated sodium channels provide the initial driving force for action potential generation and are thus essential components governing neuronal excitability. Nine different mammalian sodium channel α-subunit isoforms (Nav1.1-1.9) have been characterized to date and exhibit differential distribution and pharmacological profiles (Catterall et al., 2005). Multiple studies implicate the peripheral isoforms (Nav1.7, Nav1.8 and Nav1.9) as playing crucial roles in inflammatory and neuropathic pain mechanisms (Lai et al., 2002; Cummins et al., 2004; Priest et al., 2005). As such, sodium channel modulators are attractive candidates for the treatment of disorders of neuronal hyperexcitability such as neuropathic pain. Most clinically relevant sodium channel inhibitors are small molecules (local anesthetics, anticonvulsants) that interact with residues in the channel pore to inhibit channel function, thereby reducing neuronal excitability (England and de Groot, 2009). However, many of the currently available sodium channel inhibitors are non-selective between different isoforms, resulting in undesirable cardiac and central nervous system side effects, limiting their therapeutic window and effectiveness. Consequently, more selective pharmacological agents targeting the abnormal activity associated with specific isoforms are needed.

Paroxysmal extreme pain disorder (PEPD) and inherited erythromelalgia (IEM) arise from gain-of-function mutations in Nav1.7. Although both of these disorders are characterized by severe pain, they exhibit distinct phenotypes with differential effects on Nav1.7 channel properties. PEPD is characterized by severe rectal, ocular and submandibular pain (Fertleman et al., 2007), whereas IEM is associated with burning pain, erythema and swelling in the hands and feet (Waxman and Dib-Hajj, 2005). Furthermore, although both disorders are associated with neuronal hyperexcitability (Rush et al., 2006; Dib-Hajj et al., 2008), PEPD mutations preferentially destabilize channel inactivation

Molecular Pharmacology Fast Forward. Published on July 25, 2011 as DOI: 10.1124/mol.111.072751
This article has not been copyedited and formatted. The final version may differ from this version.

(Fertleman et al., 2006; Jarecki et al., 2008; Theile et al., 2011) whereas IEM mutations primarily enhance channel activation and slow deactivation (Cummins et al., 2004; Dib-Hajj et al., 2005; Theile et al., 2011).

Resurgent currents, first observed in cerebellar Purkinje neurons (Raman and Bean, 1997) and present in dorsal root ganglion (DRG) neurons (Cummins et al., 2005), arise following relief of ultra-fast open-channel block, believed to be mediated by the intracellular C-terminal portion of the auxiliary Navβ4 subunit (Grieco et al., 2005; Bant and Raman, 2010). PEPD mutations and other mutations which impair channel fast-inactivation exhibit enhanced resurgent currents (Jarecki et al., 2010; Theile et al., 2011). In the cerebellum, resurgent currents are believed to facilitate high-frequency firing by providing a depolarizing input near activation threshold in addition to accelerating recovery from inactivation (Raman and Bean, 1997; Khaliq et al., 2003). Indeed, computer modeling studies suggest that impaired inactivation characteristic of PEPD mutations coupled with enhanced resurgent currents increases neuronal excitability (Jarecki et al., 2010). Thus resurgent currents may contribute to increased neuronal excitability and pain associated with PEPD.

Many small molecule sodium channel inhibitors exhibit state- and use-dependent binding, typically with higher affinity to the open or inactivated channel conformations. As such, we hypothesize that because resurgent currents arise following transition to a unique channel conformation (open-channel block), it may be possible to develop small molecules capable of selectively targeting resurgent currents. Furthermore, most PEPD but only a few IEM patients respond favorably to pain treatment with carbamazepine (Dib-Hajj et al., 2007; Fertleman et al., 2007; Fischer et al., 2009). As enhanced resurgent currents are observed with PEPD mutations, but not IEM (Theile et al., 2011), we speculated that the clinical

effectiveness of carbamazepine in PEPD might be due in part to the selective manifestation and resultant inhibition of resurgent currents in PEPD, but not IEM mutant channels.

In this study, we used whole-cell patch clamp electrophysiology to investigate the effects of three sodium channel inhibitors (carbamazepine, riluzole and anandamide) on Nav1.7 wild-type and PEPD mutant (T1464I and M1627K) channels stably expressed in HEK293 cells. Carbamazepine was chosen because of it clinical usefulness in treating pain associated with PEPD (Fertleman et al., 2007), riluzole because it may preferentially inhibit persistent sodium currents (Urbani and Belluzzi, 2000) and anandamide because it may have a different mechanisms of action from classic sodium channel modulators (Bendahhou et al., 1997). Specifically, we investigated the effects of these drugs on Navβ4 peptide-mediated resurgent currents in relation to their effects on fast classical transient sodium currents and several properties associated with channel inactivation. The results from this study suggest that drugs which are effective at reducing persistent sodium currents and accelerating the rate of open-state fast-inactivation may also be good candidates for inhibiting resurgent currents.

Molecular Pharmacology Fast Forward. Published on July 25, 2011 as DOI: 10.1124/mol.111.072751
This article has not been copyedited and formatted. The final version may differ from this version.

Methods

Preparation of stably transfected cell lines. Mutations were inserted into the plasmid encoding Nav1.7 (Klugbauer et al., 1995) using the QuikChange II XL site-directed mutagenesis kit (Stratagene, La Jolla, CA, USA). HEK293 cells were grown under standard tissue culture conditions (5% CO_2; 37°C) in Dulbecco's modified Eagle's medium supplemented with 10% fetal bovine serum. Stable cell lines expressing human Nav1.7 (Nav1.7 wild-type (WT), M1627K and T1464I) channels were generated in HEK293 cells using the calcium phosphate precipitation transfection technique and antibiotic selection. The calcium phosphate–DNA mixture was added to the cell culture medium and left for 15–20 hr, after which time the cells were washed with fresh medium. After 48 hr, antibiotic (G418, Geneticin; Life Technologies, Gaithersburg, MD) was added to select for neomycin-resistant cells and establish stable cell lines. After approximately 3 weeks in G418, colonies were picked, split, and subsequently tested for channel expression using whole-cell patch-clamp recording techniques. Occasionally, HEK293 cells were grown at 28°C overnight in order to increase channel density in the cytoplasmic membrane (possibly due to enhanced trafficking or increased protein stability).

Whole-cell patch clamp recordings. Whole-cell patch clamp recordings were conducted at room temperature (~22°C) after obtaining a gigaohm seal using a HEKA EPC-10 amplifier. Data were acquired on a Windows-based Pentium IV computer using the Pulse program (v. 8.80, HEKA Electronik). Fire-polished electrodes (1.0-1.6 MΩ) were fabricated from 1.7 mm capillary glass (VWR International, West Chester, PA) using a Sutter P-97 puller (Novato, CA). A cesium-aspartate dominant intracellular solution consisted of (in mM): 20 CsCl, 100 Cs-Asp, 10 NaCl, 4 HEPES, 4 EGTA, 0.4 $CaCl_2$, 2 Mg-ATP, 0.3 Li-GTP, pH 7.3

Molecular Pharmacology Fast Forward. Published on July 25, 2011 as DOI: 10.1124/mol.111.072751
This article has not been copyedited and formatted. The final version may differ from this version.

(adjusted with CsOH). This cesium-aspartate solution was more stable in our hands than solutions with just cesium-chloride and theoretically avoided some of the effects on second messenger systems that can reportedly occur with cesium-fluoride solutions. The standard bathing solution consisted of (in mM): 140 NaCl, 1 $MgCl_2$, 3 KCl, 1 $CaCl_2$, 10 HEPES, 10 Glucose, pH 7.3 (adjusted with NaOH). For population data, cells were recorded from 35 mm plastic culture dishes bathed in 2 mL of bathing solution. Cells were recorded in the presence of dimethyl sulfoxide (DMSO; 0.1% v/v), carbamazepine, riluzole or anandamide. The drugs were added prior to recording and multiple cells were recorded from each dish. Only one drug was tested per cell. For the paired data, cells were recorded from laminin-coated glass coverslips bathed in 300 µl of bath solution. Cells were first recorded in the absence of any drug to serve as a baseline. The drugs were then added to the bath compartment by first withdrawing 30 µl of bath solution, and then adding 30 µl of 10-fold concentrated drug and mixing 10 times with a 30 µl pipette over the period of 1-2 min before recordings were repeated. Only one cell was recorded per coverslip. Voltage errors were minimized (<5 mV) using 70-80% series resistance compensation during voltage-clamp recordings. Passive leak currents were linearly cancelled by digital P/-5 subtraction. Cells were held at a membrane potential of -80 mV, and 50 ms conditioning pre-pulses to -100 mV (M1627K and T1464I) or -120 mV (WT) preceded the start of current-voltage (I/V) and resurgent current protocols to ensure increased availability of channels. The voltage protocols were conducted in the same order at the same time points for every cell, thus controlling for possible time-dependent shifts in the channel properties. Membrane currents were filtered at 5 kHz and sampled at 10-20 kHz. Data were not recorded before three minutes after whole-cell access to allow adequate time for the intracellular recording solution to equilibrate into the cell. The duration of data recordings were kept to less than 15 min

Molecular Pharmacology Fast Forward. Published on July 25, 2011 as DOI: 10.1124/mol.111.072751
This article has not been copyedited and formatted. The final version may differ from this version.

(again to minimize time dependent effects on channel properties) and cells were not held in the standard bathing solution for more than 90 min.

Chemicals and Solutions. DMSO, carbamazepine, riluzole and anandamide were obtained from Sigma-Aldrich (St. Louis, MO). A 75 mM solution of carbamazepine was made up in DMSO. A 2.67 µl aliquot was taken directly from this stock and put into the 2 ml of bathing solution for the population data to obtain a final concentration of 100 µM (DMSO ~0.1% v/v). Similarly, a 22.5 mM solution of riluzole was made up in DMSO with a final bath concentration of 30 µM. A 3.75 mM anandamide stock was made up in DMSO with a final bath concentration of 5 µM. To serve as a control against each drug in the population data, cells were recorded from in the presence of DMSO alone (2.67 µl, ~0.1% v/v). For the paired data, the final concentrations were obtained with a 10-fold stock in bath solution obtained from a dilution of the initial DMSO stock. Each cell served as its own control in the paired data experiments. In a separate set of control experiments, addition of DMSO up to ~0.3% v/v had negligible effects on the functional properties of Nav1.7 currents (data not shown).

Resurgent current analysis. In HEK293 cells, resurgent currents are only observed with inclusion of the C-terminal portion of the Navβ4 subunit (Navβ4 peptide) (Theile et al., 2011). Therefore, to generate Nav1.7-mediated resurgent currents, the Navβ4 peptide (KKLITFILKKTREK-*OH* (Biopeptide Co., San Diego, CA); 10 mM stock in ddH_2O; 100 µM final concentration) was included in the intracellular solution.

In order to maximize the signal/noise ratio necessary to detect resurgent currents, we preferentially recorded from cells that expressed larger currents (>300 pA). For all cells identified with resurgent current in this study, maximal peak resurgent currents were produced within a window of repolarization potentials from 0 mV to -30 mV and were first observed around +10 mV. These currents display unique gating kinetics with a noticeably

Molecular Pharmacology Fast Forward. Published on July 25, 2011 as DOI: 10.1124/mol.111.072751
This article has not been copyedited and formatted. The final version may differ from this version.

slow onset and decay phase, unlike classic sodium tail currents which are observed instantaneously during hyperpolarizing steps and decay rapidly. Additionally, resurgent currents display a distinctly non-monotonic I/V relationship whereas simple tail currents display a linear I/V relationship. Currents which did not meet both of these criteria were not classified as resurgent currents and therefore were excluded from the analysis of resurgent currents. Resurgent current amplitudes were measured after 1.5 ms into the repolarizing test pulse in order to avoid contamination from tail currents and were measured relative to the leak subtracted baseline. Resurgent current traces represent an average of 3 sweeps at each repolarization potential. The relative resurgent currents amplitudes were calculated by dividing the peak resurgent currents by the average peak transient current and reported as a percentage of the peak transient current. For the population data, the peak transient currents were calculated by measuring the average current elicited at +20 mV from I/V recordings obtained immediately before and after the resurgent current protocol. For the paired data, the peak transient current was measured prior to the resurgent current protocol. The test potential of +20 mV was selected for calculation of the peak transient current amplitude because the I/V relationship is linear for each of the Nav1.7 constructs at this voltage and is thus less subject to voltage-clamp errors. The average resurgent current amplitude for each Nav1.7 construct was calculated using only data from cells in which resurgent currents were detected.

Data analysis. Data were analyzed using the Pulsefit (v. 8.80, HEKA Elektronic, Germany), Origin (v. 8.0, OriginLab Corp., Northhampton, MA), and Microsoft Excel software programs. Currents were analyzed in PulseFit and filtered at 1 kHz to reduce noise. Decay time constants for open-channel fast inactivation were measured from I/V traces at +20 mV and fit to a single-exponential. The midpoints of activation and inactivation were determined

Molecular Pharmacology Fast Forward. Published on July 25, 2011 as DOI: 10.1124/mol.111.072751
This article has not been copyedited and formatted. The final version may differ from this version.

by fitting the data with a Boltzmann function. For the data presented in Figures 3D, 4C, 5C and 6C, each data point represents the average drug-mediated change normalized to DMSO for that channel construct. All channel constructs for all drug treatments are shown in these data panels. A good correlation is defined here as $R^2 > 0.5$. All data are shown as means $\pm$ S.E.M. Statistical significance was assessed with student's paired or unpaired *t* test where mentioned (* or † $p < 0.05$).

Molecular Pharmacology Fast Forward. Published on July 25, 2011 as DOI: 10.1124/mol.111.072751
This article has not been copyedited and formatted. The final version may differ from this version.

Results

Sodium channel inhibitors differentially affect resurgent currents from Nav1.7 wild-type and PEPD mutant channels. The goal of this study is to determine the effect of carbamazepine, riluzole and anandamide on Nav1.7 resurgent currents, and compare the relative effects on resurgent currents to those of other sodium channel gating properties. Due to the extended length of time needed to run the series of voltage protocols, we elected to compare data recorded from a group of cells in the absence of any of the drugs to another group of cells with each of the drugs. This approach avoids problems associated with time-dependent shifts. All three sodium channel inhibitors were dissolved in DMSO, so therefore we initially characterized the electrophysiological properties of the Nav1.7 wild-type (WT) and PEPD mutant (T1464I and M1627K) channels in the presence of DMSO alone (0.1% v/v). Table 1 shows that in accordance with our previous data (Theile et al., 2011), under these conditions the PEPD mutant channels display no difference in the voltage-dependence of activation compared to WT. However, both PEPD channels display a dramatic depolarizing shift in the $V_{1/2}$ of fast inactivation (defined as the voltage at which 50% of the channel population has transitioned to a non-conducting state) compared to WT, with the M1627K mutation exhibiting the largest shift. As can be seen in the representative whole-cell sodium currents in Figure 1, the PEPD mutations display noticeable slowing of the current decay compared to WT. Also, as demonstrated previously (Theile et al., 2011), all the constructs display prominent resurgent currents in the presence of the Navβ4 peptide, with the PEPD mutants exhibiting enhanced resurgent currents (measured as a percentage of the peak transient current) relative to WT (Fig. 1D). When the Navβ4 peptide was not included in the intracellular solution, resurgent currents were not observed (Fig. 1A, right column). The

Molecular Pharmacology Fast Forward. Published on July 25, 2011 as DOI: 10.1124/mol.111.072751
This article has not been copyedited and formatted. The final version may differ from this version.

results obtained with DMSO (0.1% v/v) in the extracellular solution are similar to that obtained previously in the absence of DMSO (Theile et al., 2011).

We next investigated the effects of carbamazepine, riluzole and anandamide on resurgent currents for each construct (Fig. 2). Carbamazepine is a classical antiepileptic drug, which has demonstrated efficacy in treating non-epileptic disorders, including myotonia, bipolar affective disorders and neuropathic pain (Rogawski and Loscher, 2004). Application of carbamazepine (100 μM) did not elicit a discernible effect on resurgent currents for the WT channel but did produce a large reduction in resurgent current amplitude for M1627K (p<0.01) and a smaller reduction for T1464I that approached significance (p=0.052). We tested a higher concentration (200 μM). Due to solubility issues, the control experiments were necessarily repeated for this data set with a higher level of DMSO (0.26% v/v) in the bath. At 200 μM carbamazepine we observed a significant reduction in resurgent current amplitude for WT, T1464I and M1627K compared to the DMSO control.

Riluzole is a neuroprotective agent mainly used in the treatment of amyotrophic lateral sclerosis (Bensimon et al., 1994), however it also displays anticonvulsant and antiepileptic properties (Romettino et al., 1991; Zgrajka et al., 2010). Riluzole has been shown to have higher affinity for persistent sodium currents compared to transient currents in cortical and cardiac tissue preparations (Urbani and Belluzzi, 2000; Weiss et al., 2010). We investigated the effects of 30 μM riluzole, a concentration which produces noticeable inhibition of tetrodotoxin-sensitive currents in DRG neurons (Song et al., 1997). Application of riluzole significantly reduced resurgent current amplitude in all three constructs, although it appeared to be most effective for WT and T1464I which demonstrated approximately 55% and 43% inhibition, respectively, when normalized to DMSO controls.

Molecular Pharmacology Fast Forward. Published on July 25, 2011 as DOI: 10.1124/mol.111.072751
This article has not been copyedited and formatted. The final version may differ from this version.

Anandamide is an endogenous cannabinoid that has demonstrated analgesic properties in animal models of pain (Calignano et al., 1998), although these effects are primarily attributable to actions on peripheral cannabinoid receptors (CB_1 and CB_2). However more recent reports suggest that anandamide inhibits sodium channels in the brain (Nicholson et al., 2003) as well as in DRG neurons independent of CB_1 and CB_2 receptors (Kim et al., 2005). Here, we investigated the effects of 5 μM anandamide on resurgent currents and observed that anandamide produced robust inhibition to a similar degree (~50%) in all three constructs.

The inhibition of resurgent currents is not correlated with effects on steady-state fast inactivation. We next examined the effects of the three drugs on the voltage-dependence of steady-state fast inactivation. Many typical sodium channel inhibitors bind with higher affinity to the inactivated states of the channel, resulting in stabilization of inactivation, as manifested in a hyperpolarizing shift in the voltage-dependence of steady-state fast inactivation. As seen in Figure 3, carbamazepine (100 μM) has no effect on steady-state fast inactivation for WT, but produces small but significant hyperpolarizing shifts in the voltage-dependence for both of the PEPD mutant constructs. At 200 μM, carbamazepine does induce a significant leftward shift for the WT construct (data not shown). Riluzole (30 μM) produces approximately a -30 mV shift in the voltage-dependence of inactivation in all three constructs. Anandamide (5 μM) also produces a hyperpolarizing shift in the voltage-dependence of inactivation for all three constructs, but appears to have the largest effect with the WT construct (~-17 mV shift relative to DMSO). Upon observing the relative shifts in the voltage-dependence of inactivation for each of the three drugs across the three channel constructs, we questioned whether there was a correlation between the degree of resurgent current inhibition by these drugs and the relative shifts in the voltage-

Molecular Pharmacology Fast Forward. Published on July 25, 2011 as DOI: 10.1124/mol.111.072751
This article has not been copyedited and formatted. The final version may differ from this version.

dependence of inactivation. To address this question, we plotted the average normalized values of the resurgent current amplitude (relative to DMSO) against the shift in the $V_{1/2}$ of inactivation (relative to DMSO) (Figure 3D). Fitting a trendline to this plot shows that there is not a good correlation ($R^2 = 0.27$) between resurgent current inhibition and the drug-induced shift in $V_{1/2}$ of inactivation.

Nav1.7-PEPD mutant channels exhibit less use-dependent inhibition compared to wild-type. We next examined the use-dependent effects of the three sodium channel inhibitors on WT and mutant channels. We employed a step-depolarization protocol from a holding potential of -80 mV to a test potential of +30 mV at a frequency of 10 Hz for a total of 20 pulses. At this frequency, noticeable use-dependent block (~25% inhibition) has been observed for carbamazepine for Nav1.2 currents (Ragsdale et al., 1991). In the absence of any of the three drugs, WT currents exhibit a progressive decrease in amplitude during the stimulus train (Figure 4A, B), indicative of increased accumulation of the channels into the inactivated state. Similar to that reported with the PEPD-V1298F mutation (Estacion et al., 2010), under control conditions both PEPD mutant channels show very little reduction of current over the length of the stimulus train, suggesting minimal accumulation of channels into the inactivated state. As seen in Figure 4A, all three drugs exhibit substantial use-dependent inhibition for WT currents, as measured by the amplitude of the last pulse of the stimulus train relative to the first pulse. Both PEPD mutant channels exhibit modest, yet significant ($p < 0.05$), use-dependent inhibition in the presence of all three drugs, with the T1464I construct appearing to be the most resistant to use-dependent block. Plotting the average normalized values of the resurgent current amplitude (relative to DMSO) against the use-dependent inhibition (relative to DMSO), shows that there is no correlation ($R^2 = 0.02$) between the two parameters.

Molecular Pharmacology Fast Forward. Published on July 25, 2011 as DOI: 10.1124/mol.111.072751
This article has not been copyedited and formatted. The final version may differ from this version.

Comparison of inhibition of resurgent current amplitude and rate of current decay. In accordance with our previous report (Theile et al., 2011), we observed an increase in the decay time constant of the fast transient current for both PEPD mutant channels compared to the WT (Figure 5A, B). Decay time constants were measured from I/V traces at +20 mV and fit to a single-exponential. Carbamazepine (100 µM) decreased the decay time constant for M1627K only and no further change was observed at 200 µM (data not shown). Riluzole decreased the time constant significantly in the WT and M1627K constructs, but not for T1464I. Anandamide reduced the time constant for all three channel constructs. Plotting the average normalized values of the resurgent current amplitude (relative to DMSO) against the percent change in decay time constant (relative to DMSO), shows that there is a good correlation ($R^2 = 0.54$) between the two parameters.

Sodium channel blockers exhibit similar inhibition of persistent and resurgent currents. Consistent with destabilized inactivation, PEPD mutant channels also exhibit non-inactivating sodium currents, commonly referred to as persistent currents (Fertleman et al., 2006; Jarecki et al., 2008; Theile et al., 2011). Although typically comprising a very small percentage of the fast sodium current, persistent currents are believed to modulate neuronal excitability (Bean, 2007). Using a 50 ms step-pulse to +20 mV, we defined 'persistent current' as the average current amplitude during the last 5 ms of the trace and displayed this as a percentage of the peak transient current amplitude (Figure 6A, B). In WT channels, little persistent current was observed (~1% of peak) with considerably more persistent current observed in the PEPD mutant channels (~4%). Riluzole and anandamide were effective in reducing persistent current amplitude in all three constructs. Carbamazepine at 100 µM reduced persistent currents in both PEPD mutant channels, but not in the WT construct, although inhibition was observed at 200 µM (data not shown). When plotting the average

Molecular Pharmacology Fast Forward. Published on July 25, 2011 as DOI: 10.1124/mol.111.072751
This article has not been copyedited and formatted. The final version may differ from this version.

normalized values of the resurgent current amplitude (relative to DMSO) against the normalized persistent current amplitude (relative to DMSO), we observed a strong correlation (R^2 = 0.85) between the two parameters.

Anandamide inhibits resurgent current with little effect on peak transient current amplitude compared to carbamazepine and riluzole. In the population experimental data set we were unable to directly compare drug-mediated effects on peak fast current amplitude to those on resurgent current amplitudes. Therefore, we next investigated the effects of the three drugs on peak fast current amplitude and resurgent current amplitude by conducting recordings from individual cells before and after drug application (Figure 7, Table 2). In order to minimize time-dependent shifts in voltage-dependent properties we used shortened set of voltage protocols from that used in the previous data set. Considering that application of 100 μM carbamazepine did not exhibit a significant reduction in resurgent current amplitude in either the WT or T1464I channels, we elected to test carbamazepine at 200 μM in this set of experiments. Application of carbamazepine significantly reduced both the peak fast current amplitude and the resurgent current amplitude for the WT and PEPD mutant channels. Application of riluzole (30 μM) significantly reduced resurgent current amplitude for all the channels, but only the M1627K mutant displayed a significant reduction in the peak fast current amplitude (~30% inhibition). Although the reduction in peak fast current amplitude for WT and T1464I was of similar magnitude as M1627K, it did not reach statistical significance (p = 0.055 by paired t-test for both channels). We also tested riluzole at 3 μM, a dose shown to be selective for persistent currents in cortical and cardiac sodium channels (Urbani and Belluzzi, 2000; Weiss et al., 2010). At this concentration, we did not observe any change in peak fast current or resurgent current amplitude for any channel, although we still observed a significant hyperpolarizing shift in the voltage-dependence of inactivation (Supplemental

Molecular Pharmacology Fast Forward. Published on July 25, 2011 as DOI: 10.1124/mol.111.072751
This article has not been copyedited and formatted. The final version may differ from this version.

Table 1). However, interestingly application of anandamide (5 μM) produced a robust inhibition of resurgent current amplitude with no change in the peak fast current amplitude for WT and T1464I. Significant inhibition of resurgent current was also seen for M1627K, although this was accompanied by a slight (~4% inhibition) but significant decrease in the peak fast current amplitude. Application of a lower concentration of anandamide (500 nM) did not reduce peak fast current or resurgent current amplitude for any channel (Table 2). In fact, there is a slight run-up in current amplitude for WT and T1464I at this lower concentration.

Molecular Pharmacology Fast Forward. Published on July 25, 2011 as DOI: 10.1124/mol.111.072751
This article has not been copyedited and formatted. The final version may differ from this version.

Discussion

Several clinically useful sodium channel inhibitors have demonstrated efficacy in treating neuropathic pain (Rogawski and Loscher, 2004). Here we investigated the effects of three sodium channel inhibitors on resurgent currents, which have been implicated in sensory neuron hyperexcitability associated with PEPD mutations (Jarecki et al., 2010). As the antiepileptic carbamazepine has been demonstrated to relieve pain in PEPD patients (Fertleman et al., 2007), we examined the effects of carbamazepine on resurgent currents and compared the effects to those of riluzole and anandamide, two other sodium channel inhibitors. Nav1.7-PEPD mutations result in overall destabilized channel inactivation. Thus we compared the effects of these drugs on resurgent currents and several other properties associated with channel inactivation. It should be noted that we did not perform a dose-response curve for inhibition with any of the selected drugs. Due to the number of channel constructs (3), sodium channel inhibitors (3) and electrophysiological parameters studied (6), an extensive dose-response study would not be practical. Furthermore, the primary objective of the present study was to determine whether resurgent currents can be selectively targeted and whether inhibition of resurgent currents can be predicted by actions of the drugs on other properties of channel inactivation. Our results suggest that sodium channel inhibitors which effectively target persistent currents and accelerate the rate of inactivation are likely to display enhanced efficacy towards resurgent currents.

Many typical sodium channel inhibitors bind with higher affinity to the open-inactivated state of the channel, resulting in stabilization of inactivation, as manifested in a hyperpolarizing shift in the voltage-dependence of steady-state fast inactivation. Stabilization of inactivation suggests enhanced binding of the inactivation gate to its receptor, which one

Molecular Pharmacology Fast Forward. Published on July 25, 2011 as DOI: 10.1124/mol.111.072751
This article has not been copyedited and formatted. The final version may differ from this version.

might predict would correlate with reduced binding of the resurgent current particle. Although all three drugs produced negative shifts in the $V_{1/2}$ of inactivation for the PEPD mutant channels, the extent of the drug-induced shift in the $V_{1/2}$ of inactivation does not correlate with the degree of resurgent current inhibition. Application of riluzole and anandamide at the chosen concentrations produced similar effects on resurgent current amplitude (Figure 2), yet riluzole had a much greater effect on the voltage-dependence of fast-inactivation. These discrepancies are not unreasonable if one considers that a negative shift in the voltage-dependence of inactivation mostly reflects enhanced closed state inactivation, which may not be important in resurgent current generation. We previously reported another mutation, Nav1.4-R1448P, induces a hyperpolarized $V_{1/2}$ of inactivation relative to wild-type Nav1.4, yet dramatically enhanced resurgent currents (Jarecki et al., 2010). Here, and as reported previously (Theile et al., 2011), we show that the T1464I mutation results in larger resurgent currents than the M1627K mutation despite having a $V_{1/2}$ of inactivation that is hyperpolarized (by ~12 mV) relative to that of the M1627K mutation. Overall these data indicate that enhancing closed-state inactivation is unlikely to directly modulate the mechanism underlying resurgent current generation.

We also found that use-dependent inhibition was not correlated with inhibition of resurgent current amplitude. Use- or state-dependent inhibition is likely the primary mechanism which allows anticonvulsants and antiepileptic drugs to be fairly well tolerated clinically: by exhibiting higher affinity for the open-inactivated channel, pathological high frequency firing results in progressive accumulation of the drug-bound channel due to the increased probability of channels in the open-inactivated state. Strong use-dependent inhibition is seen in the WT channel for all three drugs. By contrast, the degree of use-dependent drug block seen in the mutant channels, although significant, is considerably less

Molecular Pharmacology Fast Forward. Published on July 25, 2011 as DOI: 10.1124/mol.111.072751
This article has not been copyedited and formatted. The final version may differ from this version.

than that observed with WT. Carbamazepine, at a concentration within the range of therapeutic serum concentrations in clinically treated patients (Breton et al., 2005), showed ~ 40% use-dependent inhibition for WT channels and only 8% and 16% inhibition for T1464I and M1627K, respectively. PEPD mutations destabilize inactivation and exhibit enhanced recovery from inactivation (Dib-Hajj et al., 2008; Jarecki et al., 2008). Resurgent currents also facilitate recovery from inactivation (Raman and Bean, 1997; Raman and Bean, 2001). These effects likely contribute to the reduced use-dependent inhibition seen with the PEPD channels These results suggest that *use-dependent* inhibition of mutant channels may not be the primary means of pain relief in patients responsive to carbamazepine. Inhibition of WT Nav1.7 channels or reversal of other PEPD-induced changes in channel inactivation may contribute to pain relief seen with carbamazepine treatment.

We previously reported a strong correlation between the rate of current decay and resurgent current amplitude, with slower decay time constants generally resulting in larger resurgent currents (Theile et al., 2011). Consistent with that report, we demonstrate that drug-mediated acceleration of the decay time constant is correlated to drug-inhibition of resurgent current amplitude. Binding of carbamazepine is most likely too slow to increase the rate of open-channel inactivation and therefore this may be why it does not selectively inhibit resurgent currents. By contrast, we observed that application of anandamide at 5 µM (but not 500 nM) produced a strong inhibition (~60% inhibition for all three constructs) in resurgent current amplitude with little or no effect on the peak fast current amplitude. This result is especially intriguing because it demonstrates the potential feasibility of identifying or developing drugs that selectively target resurgent currents while sparing the normal fast current. Although the mechanism of selective resurgent current inhibition by anandamide is unclear, a study with Nav1.4 channels speculated that fatty acids might interact with the

Molecular Pharmacology Fast Forward. Published on July 25, 2011 as DOI: 10.1124/mol.111.072751
This article has not been copyedited and formatted. The final version may differ from this version.

voltage sensor of domain IV (Bendahhou et al., 1997). This type of interaction might be more stable than that of carbamazepine, resulting in an faster rates of inactivation and reduced resurgent currents.

We found that the resurgent current inhibition showed the strongest correlation with persistent current inhibition. PEPD mutations result in increased persistent currents compared to WT (Fig. 6), as reported elsewhere (Dib-Hajj et al., 2008; Jarecki et al., 2008; Theile et al., 2011). We observed inhibition of these currents by carbamazepine, although not to the same extent as noted previously (Fertleman et al., 2006). The T1464I and M1627K mutants displayed similar persistent current inhibition with each of the three drugs; however, carbamazepine (100 μM) was ineffective against persistent currents generated by WT channels. Despite these results, carbamazepine does not appear to selectively inhibit resurgent currents, as peak currents are also significantly attenuated. As PEPD mutations, but not IEM, give rise to large persistent currents, inhibition of persistent currents may partially explain the effectiveness of carbamazepine in PEPD but not IEM patients. As different PEPD mutants display variations in inactivation and resurgent current properties (Theile et al., 2011), the variable effectiveness of carbamazepine treatment across PEPD patients (Fertleman et al., 2007) may be a consequence of a differential sensitivity of carbamazepine to the mutations expressed by the patients. Here, we focused on just two of the ten known PEPD mutations, thus we cannot rule out selective inhibition of resurgent currents by carbamazepine in the other mutant channels.

The non-selective properties inherent to sodium channel inhibitors limit the effectiveness of these drugs in treating pain. Therefore, there is an increasing need for the development of drugs which are either isoform- or state-specific. Resurgent currents arise following the transition to a unique channel state and thus represent an interesting avenue for

the development of targeted sodium channel modulators in the treatment of pain and possibly other disorders of excitability such as epilepsy (Hargus et al., 2011). As other aspects of channel function appear to be closely associated with the mechanism of resurgent current generation, we may be able to exploit these similarities in the search for more selective agents for treating resurgent current mediated-disorders of excitability.

Molecular Pharmacology Fast Forward. Published on July 25, 2011 as DOI: 10.1124/mol.111.072751
This article has not been copyedited and formatted. The final version may differ from this version.

Acknowledgements

Thanks to James O. Jackson II for assistance in generating the stable Nav1.7 HEK293 cell lines.

Authorship Contributions

Participated in research design: Theile, Cummins

Conducted experiments: Theile

Performed data analysis: Theile

Wrote or contributed to the writing of the manuscript: Theile, Cummins

References

Bant JS and Raman IM (2010) Control of transient, resurgent, and persistent current by open-channel block by Na channel beta4 in cultured cerebellar granule neurons. *Proc Natl Acad Sci U S A* **107**:12357-12362.

Bean BP (2007) The action potential in mammalian central neurons. *Nat Rev Neurosci* **8**:451-465.

Bendahhou S, Cummins TR and Agnew WS (1997) Mechanism of modulation of the voltage-gated skeletal and cardiac muscle sodium channels by fatty acids. *Am J Physiol* **272**:C592-600.

Bensimon G, Lacomblez L and Meininger V (1994) A controlled trial of riluzole in amyotrophic lateral sclerosis. ALS/Riluzole Study Group. *N Engl J Med* **330**:585-591.

Breton H, Cociglio M, Bressolle F, Peyriere H, Blayac JP and Hillaire-Buys D (2005) Liquid chromatography-electrospray mass spectrometry determination of carbamazepine, oxcarbazepine and eight of their metabolites in human plasma. *J Chromatogr B Analyt Technol Biomed Life Sci* **828**:80-90.

Calignano A, La Rana G, Giuffrida A and Piomelli D (1998) Control of pain initiation by endogenous cannabinoids. *Nature* **394**:277-281.

Catterall WA, Goldin AL and Waxman SG (2005) International Union of Pharmacology. XLVII. Nomenclature and structure-function relationships of voltage-gated sodium channels. *Pharmacol Rev* **57**:397-409.

Cummins TR, Dib-Hajj SD, Herzog RI and Waxman SG (2005) Nav1.6 channels generate resurgent sodium currents in spinal sensory neurons. *FEBS Lett* **579**:2166-2170.

Cummins TR, Dib-Hajj SD and Waxman SG (2004) Electrophysiological properties of mutant Nav1.7 sodium channels in a painful inherited neuropathy. *J Neurosci* **24**:8232-8236.

Dib-Hajj SD, Cummins TR, Black JA and Waxman SG (2007) From genes to pain: Na v 1.7 and human pain disorders. *Trends Neurosci* **30**:555-563.

Dib-Hajj SD, Estacion M, Jarecki BW, Tyrrell L, Fischer TZ, Lawden M, Cummins TR and Waxman SG (2008) Paroxysmal extreme pain disorder M1627K mutation in human Nav1.7 renders DRG neurons hyperexcitable. *Mol Pain* **4**:37.

Dib-Hajj SD, Rush AM, Cummins TR, Hisama FM, Novella S, Tyrrell L, Marshall L and Waxman SG (2005) Gain-of-function mutation in Nav1.7 in familial erythromelalgia induces bursting of sensory neurons. *Brain* **128**:1847-1854.

England S and de Groot MJ (2009) Subtype-selective targeting of voltage-gated sodium channels. *Br J Pharmacol* **158**:1413-1425.

Estacion M, Waxman SG and Dib-Hajj SD (2010) Effects of ranolazine on wild-type and mutant hNav1.7 channels and on DRG neuron excitability. *Mol Pain* **6**:35.

Fertleman CR, Baker MD, Parker KA, Moffatt S, Elmslie FV, Abrahamsen B, Ostman J, Klugbauer N, Wood JN, Gardiner RM and Rees M (2006) SCN9A mutations in paroxysmal extreme pain disorder: allelic variants underlie distinct channel defects and phenotypes. *Neuron* **52**:767-774.

Fertleman CR, Ferrie CD, Aicardi J, Bednarek NA, Eeg-Olofsson O, Elmslie FV, Griesemer DA, Goutieres F, Kirkpatrick M, Malmros IN, Pollitzer M, Rossiter M, Roulet-Perez E, Schubert R, Smith VV, Testard H, Wong V and Stephenson JB (2007) Paroxysmal

extreme pain disorder (previously familial rectal pain syndrome). *Neurology* **69**:586-595.

Fischer TZ, Gilmore ES, Estacion M, Eastman E, Taylor S, Melanson M, Dib-Hajj SD and Waxman SG (2009) A novel Nav1.7 mutation producing carbamazepine-responsive erythromelalgia. *Ann Neurol* **65**:733-741.

Grieco TM, Malhotra JD, Chen C, Isom LL and Raman IM (2005) Open-channel block by the cytoplasmic tail of sodium channel beta4 as a mechanism for resurgent sodium current. *Neuron* **45**:233-244.

Hargus NJ, Merrick EC, Nigam A, Kalmar CL, Baheti AR, Bertram EH, 3rd and Patel MK (2011) Temporal lobe epilepsy induces intrinsic alterations in Na channel gating in layer II medial entorhinal cortex neurons. *Neurobiol Dis* **41**:361-376.

Jarecki BW, Piekarz AD, Jackson JO, 2nd and Cummins TR (2010) Human voltage-gated sodium channel mutations that cause inherited neuronal and muscle channelopathies increase resurgent sodium currents. *J Clin Invest* **120**:369-378.

Jarecki BW, Sheets PL, Jackson JO, 2nd and Cummins TR (2008) Paroxysmal extreme pain disorder mutations within the D3/S4-S5 linker of Nav1.7 cause moderate destabilization of fast inactivation. *J Physiol* **586**:4137-4153.

Khaliq ZM, Gouwens NW and Raman IM (2003) The contribution of resurgent sodium current to high-frequency firing in Purkinje neurons: an experimental and modeling study. *J Neurosci* **23**:4899-4912.

Kim HI, Kim TH, Shin YK, Lee CS, Park M and Song JH (2005) Anandamide suppression of Na+ currents in rat dorsal root ganglion neurons. *Brain Res* **1062**:39-47.

Klugbauer N, Lacinova L, Flockerzi V and Hofmann F (1995) Structure and functional expression of a new member of the tetrodotoxin-sensitive voltage-activated sodium channel family from human neuroendocrine cells. *EMBO J* **14**:1084-1090.

Lai J, Gold MS, Kim CS, Bian D, Ossipov MH, Hunter JC and Porreca F (2002) Inhibition of neuropathic pain by decreased expression of the tetrodotoxin-resistant sodium channel, NaV1.8. *Pain* **95**:143-152.

Nicholson RA, Liao C, Zheng J, David LS, Coyne L, Errington AC, Singh G and Lees G (2003) Sodium channel inhibition by anandamide and synthetic cannabimimetics in brain. *Brain Res* **978**:194-204.

Priest BT, Murphy BA, Lindia JA, Diaz C, Abbadie C, Ritter AM, Liberator P, Iyer LM, Kash SF, Kohler MG, Kaczorowski GJ, MacIntyre DE and Martin WJ (2005) Contribution of the tetrodotoxin-resistant voltage-gated sodium channel NaV1.9 to sensory transmission and nociceptive behavior. *Proc Natl Acad Sci U S A* **102**:9382-9387.

Ragsdale DS, Scheuer T and Catterall WA (1991) Frequency and voltage-dependent inhibition of type IIA Na+ channels, expressed in a mammalian cell line, by local anesthetic, antiarrhythmic, and anticonvulsant drugs. *Mol Pharmacol* **40**:756-765.

Raman IM and Bean BP (1997) Resurgent sodium current and action potential formation in dissociated cerebellar Purkinje neurons. *J Neurosci* **17**:4517-4526.

Raman IM and Bean BP (2001) Inactivation and recovery of sodium currents in cerebellar Purkinje neurons: evidence for two mechanisms. *Biophys J* **80**:729-737.

Rogawski MA and Loscher W (2004) The neurobiology of antiepileptic drugs for the treatment of nonepileptic conditions. *Nat Med* **10**:685-692.

Romettino S, Lazdunski M and Gottesmann C (1991) Anticonvulsant and sleep-waking influences of riluzole in a rat model of absence epilepsy. *Eur J Pharmacol* **199**:371-373.

Rush AM, Dib-Hajj SD, Liu S, Cummins TR, Black JA and Waxman SG (2006) A single sodium channel mutation produces hyper- or hypoexcitability in different types of neurons. *Proc Natl Acad Sci U S A* **103**:8245-8250.

Song JH, Huang CS, Nagata K, Yeh JZ and Narahashi T (1997) Differential action of riluzole on tetrodotoxin-sensitive and tetrodotoxin-resistant sodium channels. *J Pharmacol Exp Ther* **282**:707-714.

Theile JW, Jarecki BW, Piekarz AD and Cummins TR (2011) Nav1.7 mutations associated with paroxysmal extreme pain disorder, but not erythromelalgia, enhance Nav{beta}4 peptide-mediated resurgent sodium currents. *J Physiol* **589**:597-608.

Urbani A and Belluzzi O (2000) Riluzole inhibits the persistent sodium current in mammalian CNS neurons. *Eur J Neurosci* **12**:3567-3574.

Waxman SG and Dib-Hajj S (2005) Erythermalgia: molecular basis for an inherited pain syndrome. *Trends Mol Med* **11**:555-562.

Weiss S, Benoist D, White E, Teng W and Saint DA (2010) Riluzole protects against cardiac ischaemia and reperfusion damage via block of the persistent sodium current. *Br J Pharmacol* **160**:1072-1082.

Zgrajka W, Nieoczym D, Czuczwar M, Kis J, Brzana W, Wlaz P and Turski WA (2010) Evidences for pharmacokinetic interaction of riluzole and topiramate with pilocarpine in pilocarpine-induced seizures in rats. *Epilepsy Res* **88**:269-274.

Molecular Pharmacology Fast Forward. Published on July 25, 2011 as DOI: 10.1124/mol.111.072751
This article has not been copyedited and formatted. The final version may differ from this version.

FOOTNOTES

a) This work was supported by the 2010 PhRMA Foundation Post Doctoral Fellowship in Pharmacology/Toxicology Award and the National Institutes of Health National Institute of Neurological Disorders and Stroke [Grant R01NS053422].

b) Reprint requests:

Jonathan Theile

950 West Walnut Street, R2-459

Indianapolis, IN 46202, USA

E-mail: jtheile@iupui.edu

Molecular Pharmacology Fast Forward. Published on July 25, 2011 as DOI: 10.1124/mol.111.072751
This article has not been copyedited and formatted. The final version may differ from this version.

Legends for Figures

Figure 1. PEPD mutant channels exhibit differentially enhanced resurgent currents. A. I/V family traces (left column) and resurgent protocol traces recorded in the presence (middle column) and absence (right column) of Navβ4 peptide from representative HEK293 cells expressing either Nav1.7 WT or mutant channels. For the I/V traces, cells were held at -80 mV, and currents were elicited with 50 ms test pulses to potentials ranging from -80 to +60 mV. Note that the resurgent current amplitudes are scaled to reflect the relative size of resurgent currents in relation to WT. The resurgent current protocol is shown in (B). C. I/V curve for resurgent current traces from individual cells shown in the middle panel of (A). D. Resurgent current amplitude, as measured as a percentage of the average peak transient current elicited at +20 mV obtained immediately prior to and following the resurgent current protocol. Recordings were conducted in presence of DMSO alone (0.1% v/v). *$p < 0.05$ from WT by student's unpaired t-test. n = 9-10 cells each condition.

Figure 2. Differential inhibition of resurgent currents by sodium channel modulators. Resurgent current amplitudes in the presence of DMSO, carbamazepine (CBZ), riluzole (RZ) or anandamide (AEA) for Nav1.7 WT (A), T1464I (B) and M1627K (C). *$p < 0.05$ from DMSO by student's unpaired t-test. n = 7-10 cells each condition. All recordings were done with the Navβ4 peptide in the intracellular solution.

Figure 3. Sodium channel inhibitors stabilize fast inactivation. Steady-state fast inactivation curves for WT (A), T1464I (B) and M1627K (C) in the presence of the three sodium channel inhibitors. The voltage dependence of steady-state fast inactivation was

Molecular Pharmacology Fast Forward. Published on July 25, 2011 as DOI: 10.1124/mol.111.072751
This article has not been copyedited and formatted. The final version may differ from this version.

examined using a series of 200 ms conditioning pre-pulses from -120 mV to +30 mV, followed by a 20 ms test pulse to +15 mV to assess channel availability. The midpoint of activation was estimated by fitting the data with a Bolztmann function. D. The average resurgent current amplitude relative to DMSO for each channel construct at each drug concentration tested is plotted against the respective shift in the $V_{1/2}$ of inactivation relative to DMSO and fitted with a linear trendline. *n* = 7-10 cells each condition. All recordings were done with the Navβ4 peptide in the intracellular solution.

Figure 4. Use-dependent drug block is impaired in PEPD mutant channels. A. The ratio of peak WT, T1464I and M1627K currents from the first pulse to the last pulse of the 10 Hz stimulation protocol (as shown in B) in the presence of different sodium channel inhibitors. Data are presented as mean percentage of current remaining (amplitude of 20th pulse divided by amplitude of 1st pulse). B. Stimulation protocol (top panel) and sample trace from WT in presence of DMSO alone (bottom panel). C. The average resurgent current amplitude relative to DMSO for each channel construct at each drug concentration tested is plotted against the respective percent change in current remaining (as shown in A) relative to DMSO and fitted with a linear trendline. *p < 0.05 from DMSO by student's unpaired t-test. *n* = 7-10 cells each condition. All recordings were done with the Navβ4 peptide in the intracellular solution.

Figure 5. Sodium channel inhibitors accelerate the rate of current decay. A. Decay time constant values for WT, T1464I and M1627K channels in the presence of the different sodium channel modulators. B. Normalized current traces elicited by a step depolarization to +20 mV from representative WT or PEPD mutant channels as indicated by arrows. C. The

average resurgent current amplitude relative to DMSO for each channel construct at each drug concentration tested is plotted against the respective percent change in decay time constant (as shown in A) relative to DMSO and fitted with a linear trendline. *$p < 0.05$ from DMSO by student's unpaired t-test. n = 7-10 cells each condition. All recordings were done with the Navβ4 peptide in the intracellular solution.

Figure 6. Sodium channel inhibitors decrease persistent currents. A. Persistent current values for WT, T1464I and M1627K channels in the presence of the different sodium channel inhibitors. Data are presented as the mean percentage of the peak transient current. B. Normalized current traces elicited by a step depolarization to +20 mV from representative WT or PEPD mutant channels as indicated by arrows. Persistent current amplitudes were measured relative to leak-subtracted baseline and averaged over the last 5 ms of the pulse as indicated by the shaded region. C. The average resurgent current amplitude relative to DMSO for each channel construct at each drug concentration tested is plotted against the respective persistent current amplitude (as shown in A) relative to DMSO and fitted with a linear trendline. *$p < 0.05$ from DMSO by student's unpaired t-test. n = 7-10 cells each condition. All recordings were done with the Navβ4 peptide in the intracellular solution.

Figure 7. Anandamide selectively reduces resurgent current amplitude. Representative I/V and resurgent current traces for the T1464I mutant channel before and after application of carbamazepine (A), riluzole (B) and anandamide (C). All recordings were done with the Navβ4 peptide in the intracellular solution.

Molecular Pharmacology Fast Forward. Published on July 25, 2011 as DOI: 10.1124/mol.111.072751
This article has not been copyedited and formatted. The final version may differ from this version.

Tables

Table 1: Voltage-dependence of activation and steady-state fast inactivation for Nav1.7 wild-type and PEPD mutant channels.

	$V_{1/2}$ activation (mV)[a]	$V_{1/2}$ inactivation (mV)[b]	*n*
Wild-type			
DMSO (0.1% v/v)	-10.6 ± 0.8	-58.8 + 1.5	10
T1464I			
DMSO (0.1% v/v)	-11.7 ± 0.6	-49.0 ± 0.5*	9
M1627K			
DMSO (0.1% v/v)	-10.2 ± 0.6	-37.1 ± 0.5*†	10

[a]The voltage dependence of activation was examined using a series of 50 ms depolarizing test pulses from -80 mV to +60 mV. The midpoint of activation was estimated by fitting the data with a Bolztmann function. [b]The voltage dependence of steady-state fast inactivation was examined using a series of 200 ms conditioning pre-pulses from -120 mV to +30 mV, followed by a 20 ms test pulse to +15 mV to assess channel availability. The midpoint of inactivation was estimated by fitting the data with a Bolztmann function. *$p < 0.05$ from wild-type and †$p < 0.05$ from T1464I by unpaired student's t-test.

Molecular Pharmacology Fast Forward. Published on July 25, 2011 as DOI: 10.1124/mol.111.072751
This article has not been copyedited and formatted. The final version may differ from this version.

Table 2: Inhibition of peak transient and resurgent currents by sodium channel inhibitors.

	I_{peak} (nA)[a]	I_{NaR} (% I_{peak})[b]	*n*
WT			
Ctrl	-2.84 ± 0.36	4.9 ± 0.4	5
CBZ 200 µm	-2.14 ± 0.22*	3.8 ± 0.2*	
Ctrl	-5.45 ± 2.48	4.1 ± 0.7	6
RZ 30 µm	-3.77 ± 1.81	2.2 ± 0.2*	
Ctrl	-2.63 ± 0.57	5.3 ± 1.0	4
RZ 3 µm	-2.76 ± 0.59	5.4 ± 1.2	
Ctrl	-4.01 ± 0.73	4.6 ± 0.9	6
AEA 5 µM	-3.89 ± 0.75	2.1 ± 0.3*	
Ctrl	-7.02 ± 2.17	3.7 ± 0.07	5
AEA 500 nM	-8.22 ± 2.9	4.3 ± 0.6*	
T1464I			
Ctrl	-1.84 ± 0.36	14.9 ± 1.1	6
CBZ 200 µm	-1.55 ± 0.30*	11.1 ± 0.8*	
Ctrl	-2.24 ± 0.6	15.1 ± 1.9	5
RZ 30 µm	-1.59 ± 0.47	9.0 ± 0.6*	
Ctrl	-2.02 ± 0.59	17.4 ± 2.7	4
RZ 3 µm	-2.21 ± 0.64	17.9 ± 3.1	
Ctrl	-1.26 ± 0.17	18.6 ± 0.9	5
AEA 5 µM	-1.30 ± 0.18	7.0 ± 1.2*	
Ctrl	-1.35 ± 0.5	19.0 ± 2.3	5
AEA 500 nM	-1.42 ± 0.53*	18.7 ± 2.1	
M1627K			
Ctrl	-1.04 ± 0.21	15.4 ± 0.6	6
CBZ 200 µm	-0.84 ± 0.17*	13.6 ± 1.0*	
Ctrl	-0.74 ± 0.17	13.5 ± 0.5	6
RZ 30 µm	-0.52 ± 0.13*	9.7 ± 0.8*	
Ctrl	-1.16 ± 0.3	12.2 ± 0.8	5
RZ 3 µm	-1.16 ± 0.32	12.3 ± 0.7	
Ctrl	-0.95 ± 0.23	12.2 ± 1.0	5
AEA 5 µM	-0.91 ± 0.23*	5.6 ± 0.8*	
Ctrl	-0.94 ± 0.16	14.2 ± 1.5	4
AEA 500 nM	-0.92 ± 0.14	14.7 ± 0.9	

[a]The peak transient current was measured at a test potential of +20 mV obtained from an I/V recording. [b]The relative resurgent currents amplitudes were calculated by dividing the peak

Molecular Pharmacology Fast Forward. Published on July 25, 2011 as DOI: 10.1124/mol.111.072751
This article has not been copyedited and formatted. The final version may differ from this version.

resurgent current by the peak transient current and represented as a percentage of the peak transient current. *$p < 0.05$ from control by paired student's t-test.

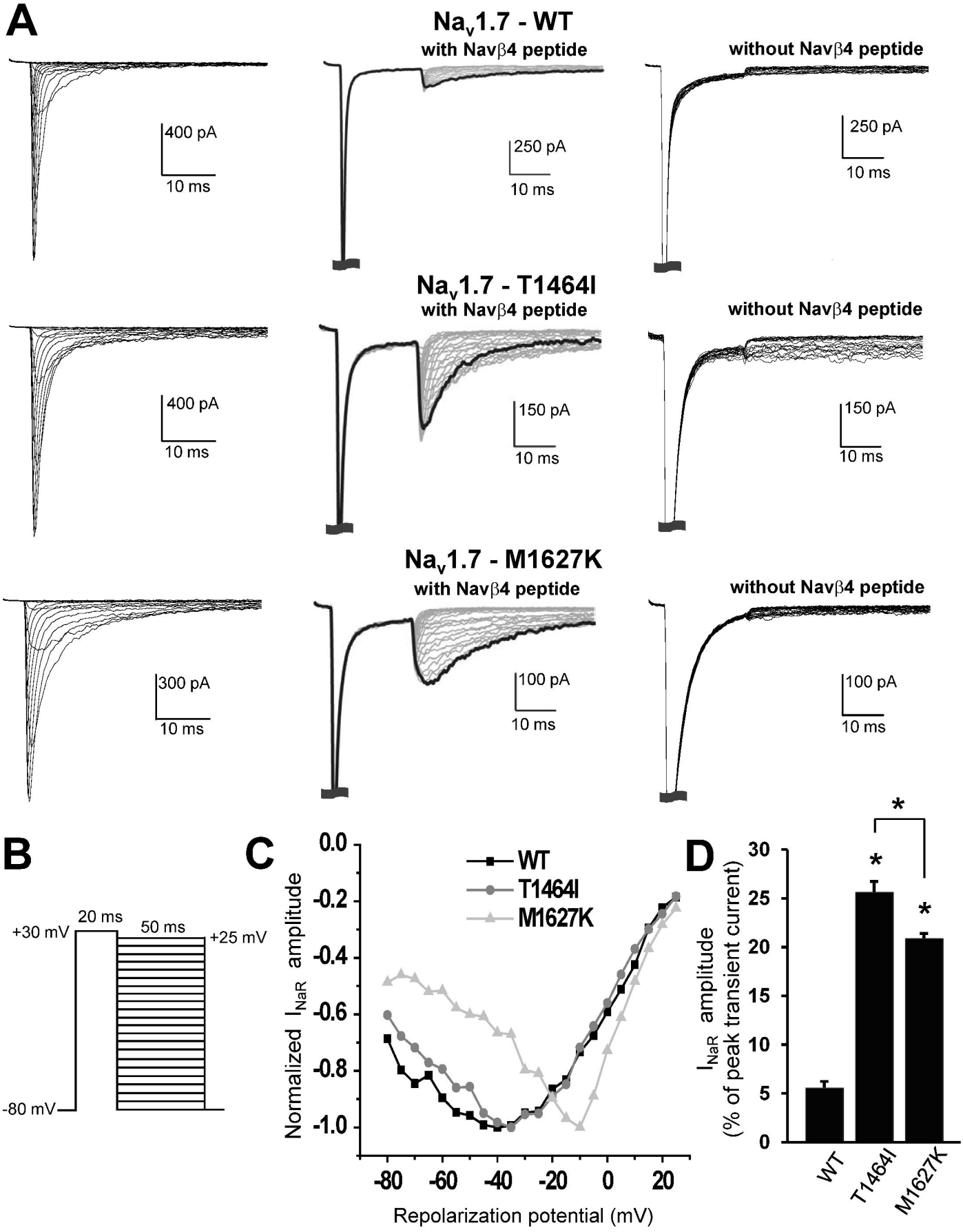
A
Na$_v$1.7 - WT
with Navβ4 peptide
without Navβ4 peptide
400 pA
10 ms
250 pA
10 ms
250 pA
10 ms
Na$_v$1.7 - T1464I
with Navβ4 peptide
without Navβ4 peptide
400 pA
10 ms
150 pA
10 ms
150 pA
10 ms
Na$_v$1.7 - M1627K
with Navβ4 peptide
without Navβ4 peptide
300 pA
10 ms
100 pA
10 ms
100 pA
10 ms
B
+30 mV
20 ms
50 ms
+25 mV
-80 mV
C
WT
T1464I
M1627K
Normalized I_{NaR} amplitude
0.0
-0.2
-0.4
-0.6
-0.8
-1.0
-80
-60
-40
-20
0
20
Repolarization potential (mV)
D
I_{NaR} amplitude
(% of peak transient current)
30
25
20
15
10
5
0
*
*
*
WT
T1464I
M1627K

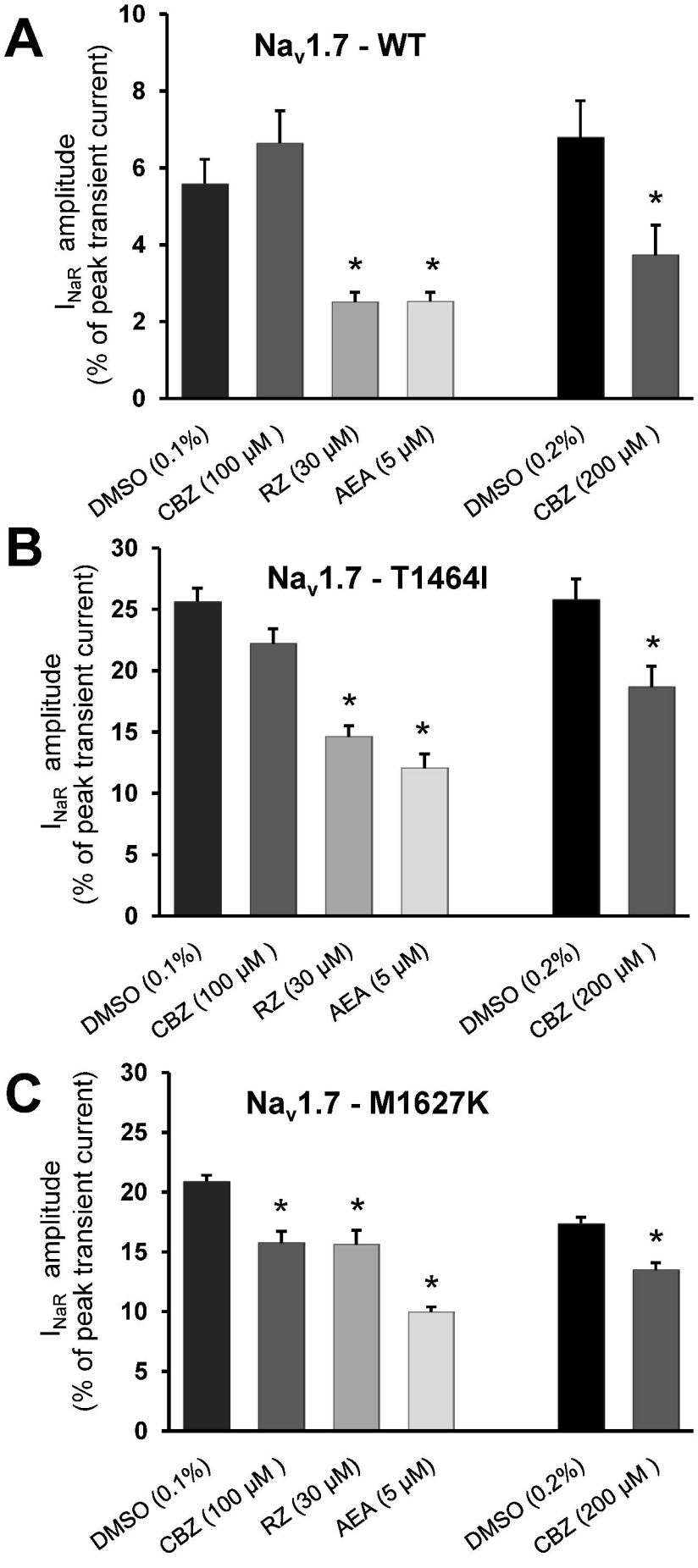
A
Na$_v$1.7 - WT
I_{NaR} amplitude
(% of peak transient current)
10
8
6
4
2
0
*
*
*
DMSO (0.1%)
CBZ (100 µM)
RZ (30 µM)
AEA (5 µM)
DMSO (0.2%)
CBZ (200 µM)
B
Na$_v$1.7 - T1464I
I_{NaR} amplitude
(% of peak transient current)
30
25
20
15
10
5
0
*
*
*
DMSO (0.1%)
CBZ (100 µM)
RZ (30 µM)
AEA (5 µM)
DMSO (0.2%)
CBZ (200 µM)
C
Na$_v$1.7 - M1627K
I_{NaR} amplitude
(% of peak transient current)
30
25
20
15
10
5
0
*
*
*
*
DMSO (0.1%)
CBZ (100 µM)
RZ (30 µM)
AEA (5 µM)
DMSO (0.2%)
CBZ (200 µM)

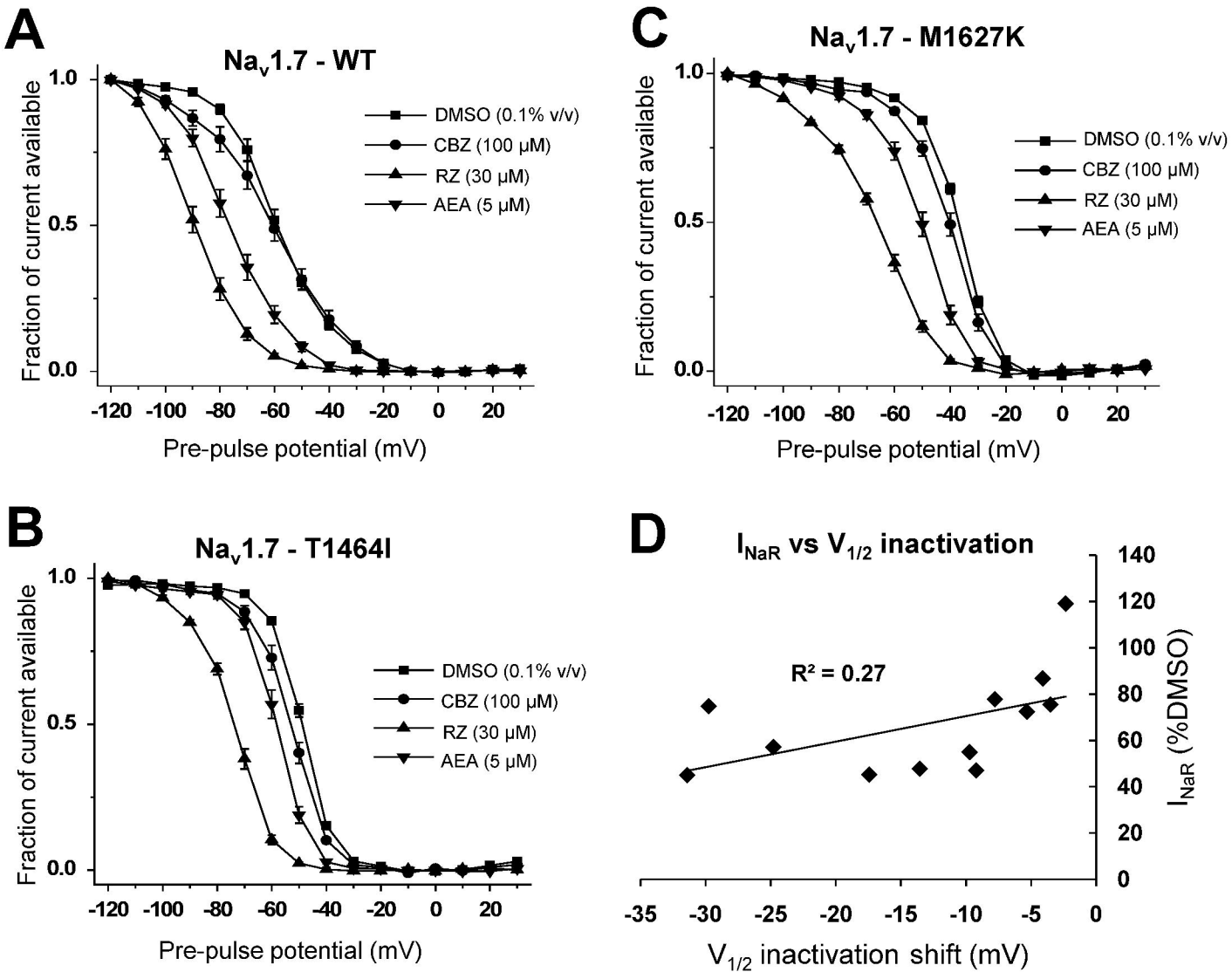
A
Na$_v$1.7 - WT
Fraction of current available
1.0
0.5
0.0
-120 -100 -80 -60 -40 -20 0 20
Pre-pulse potential (mV)
DMSO (0.1% v/v)
CBZ (100 µM)
RZ (30 µM)
AEA (5 µM)
C
Na$_v$1.7 - M1627K
Fraction of current available
1.0
0.5
0.0
-120 -100 -80 -60 -40 -20 0 20
Pre-pulse potential (mV)
DMSO (0.1% v/v)
CBZ (100 µM)
RZ (30 µM)
AEA (5 µM)
B
Na$_v$1.7 - T1464I
Fraction of current available
1.0
0.5
0.0
-120 -100 -80 -60 -40 -20 0 20
Pre-pulse potential (mV)
DMSO (0.1% v/v)
CBZ (100 µM)
RZ (30 µM)
AEA (5 µM)
D
I$_{NaR}$ vs V$_{1/2}$ inactivation
R² = 0.27
I$_{NaR}$ (%DMSO)
140
120
100
80
60
40
20
0
-35 -30 -25 -20 -15 -10 -5 0
V$_{1/2}$ inactivation shift (mV)

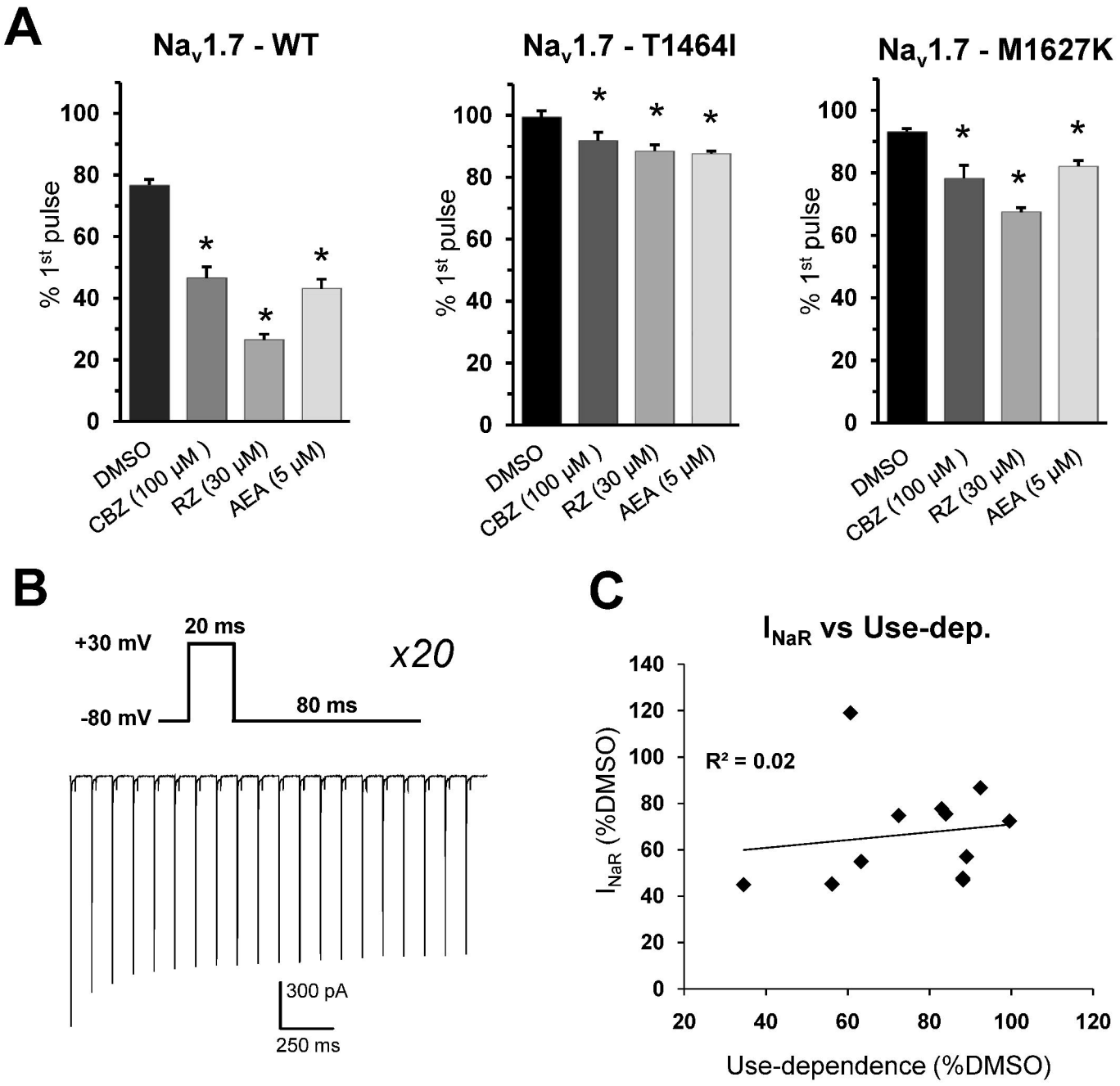
A
Na$_v$1.7 - WT
Na$_v$1.7 - T1464I
Na$_v$1.7 - M1627K
% 1st pulse
100
80
60
40
20
0
*
DMSO
CBZ (100 µM)
RZ (30 µM)
AEA (5 µM)
B
+30 mV
-80 mV
20 ms
80 ms
x20
300 pA
250 ms
C
I$_{NaR}$ vs Use-dep.
R² = 0.02
I$_{NaR}$ (%DMSO)
Use-dependence (%DMSO)
140
120
100
80
60
40
20
0

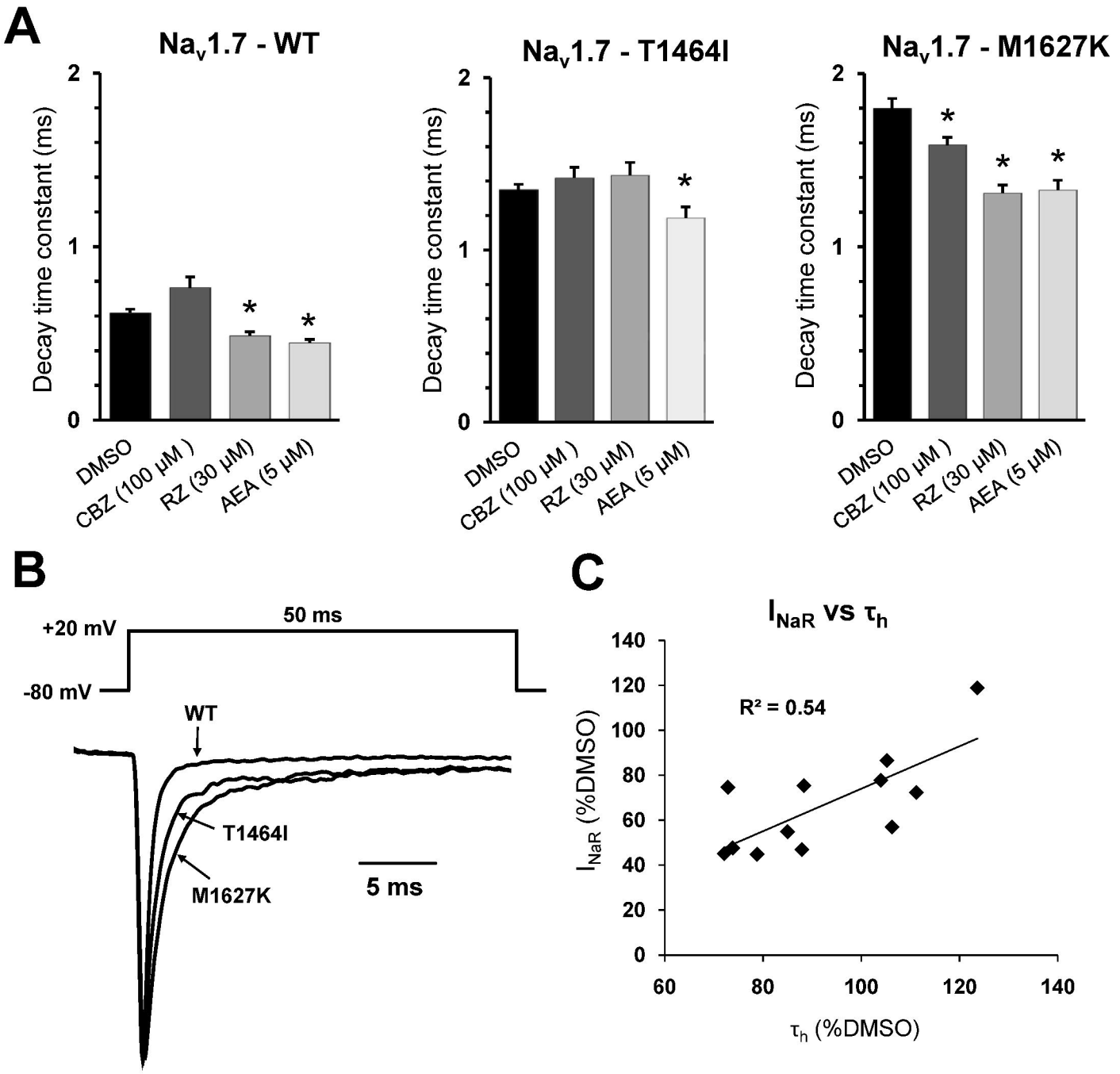
A
Na$_v$1.7 - WT
Na$_v$1.7 - T1464I
Na$_v$1.7 - M1627K
Decay time constant (ms)
2
1
0
*
DMSO
CBZ (100 µM)
RZ (30 µM)
AEA (5 µM)
B
+20 mV
-80 mV
50 ms
WT
T1464I
M1627K
5 ms
C
I$_{NaR}$ vs τ$_h$
R² = 0.54
I$_{NaR}$ (%DMSO)
τ$_h$ (%DMSO)
140
120
100
80
60
40
20
0
60
80
100
120
140

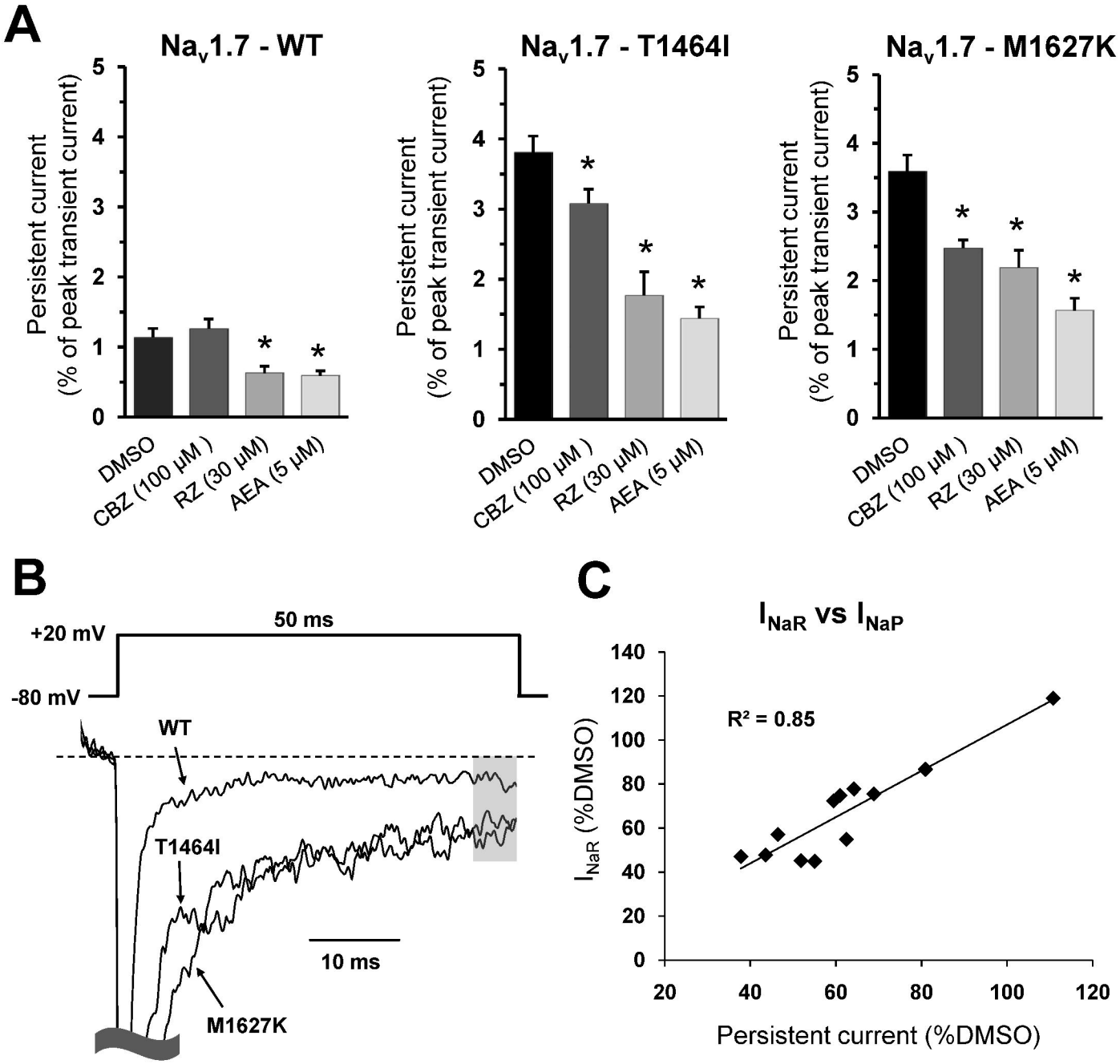
A
Na$_v$1.7 - WT
Na$_v$1.7 - T1464I
Na$_v$1.7 - M1627K
Persistent current (% of peak transient current)
DMSO
CBZ (100 µM)
RZ (30 µM)
AEA (5 µM)
B
+20 mV
-80 mV
50 ms
WT
T1464I
M1627K
10 ms
C
I$_{NaR}$ vs I$_{NaP}$
R² = 0.85
I$_{NaR}$ (%DMSO)
Persistent current (%DMSO)

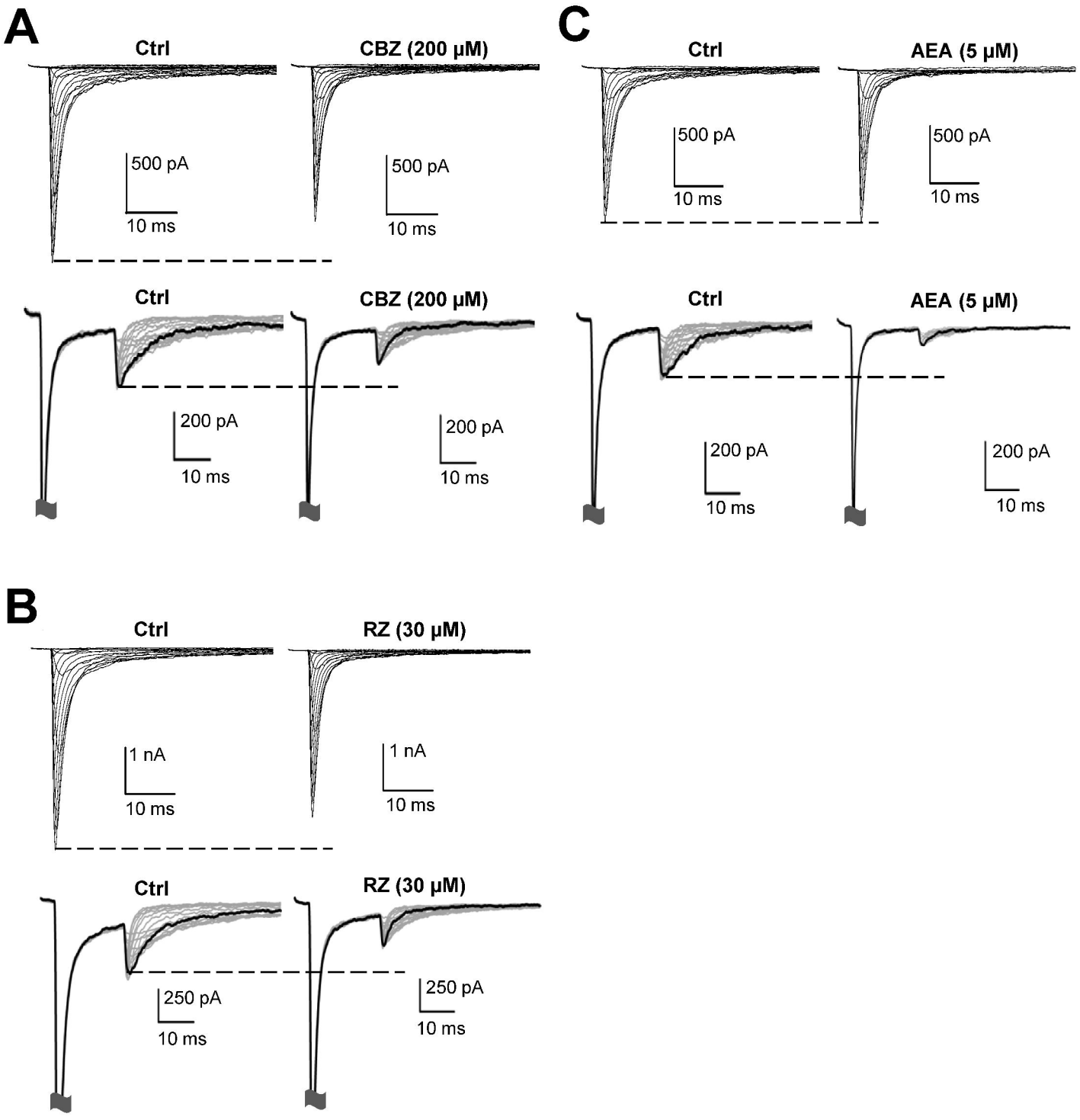
A
Ctrl
CBZ (200 µM)
500 pA
10 ms
500 pA
10 ms
Ctrl
CBZ (200 µM)
200 pA
10 ms
200 pA
10 ms
C
Ctrl
AEA (5 µM)
500 pA
10 ms
500 pA
10 ms
Ctrl
AEA (5 µM)
200 pA
10 ms
200 pA
10 ms
B
Ctrl
RZ (30 µM)
1 nA
10 ms
1 nA
10 ms
Ctrl
RZ (30 µM)
250 pA
10 ms
250 pA
10 ms

Inhibition of Navβ4 peptide-mediated resurgent sodium currents in Nav1.7 channels by carbamazepine, riluzole and anandamide

Jonathan W. Theile and Theodore R. Cummins

Molecular Pharmacology

Supplemental Table 1. Decay time constant and voltage-dependence of steady-state fast inactivation for PEPD Nav1.7 channels.

	τ_h (ms)[a]	$V_{1/2}$ inactivation (mV)[b]	*n*
WT			
Ctrl	0.83 ± 0.09	-55.2 ± 2.0	5
CBZ 200 µm	0.67 ± 0.06*	-67.1 ± 3.5*	
Ctrl	0.90 ± 0.18	-55.5 ± 3.7	6
RZ 30 µm	0.62 ± 0.06	-83.4 ± 2.0*	
Ctrl	0.64 ± 0.04	-58.4 ± 0.5	4
RZ 3 µm	0.65 ± 0.07	-65.0 ± 1.5*	
Ctrl	0.74 ± 0.03	-54.4 ± 1.1	6
AEA 5 µM	0.67 ± 0.03*	-64.5 ±2.7*	
Ctrl	0.63 ± 0.03	-57.7 ± 0.4	5
AEA 500 nM	0.66 ± 0.04*	-56.8 ± 0.7	
T1464I			
Ctrl	1.83 ± 0.08	-43.9 + 1.8	6
CBZ 200 µm	1.71 ± 0.08	-50.7 ± 2.5*	
Ctrl	1.90 ± 0.13	-48.6 ± 3.2	5
RZ 30 µm	1.27 ± 0.07*	-68.4 ± 2.7*	
Ctrl	2.02 ± 0.18	-44.0 ± 0.8	4
RZ 3 µm	1.94 ± 0.24	-47.0 ± 1.0*	
Ctrl	1.96 ± 0.14	-45.7 ± 1.3	5
AEA 5 µM	1.57 ± 0.12*	-52.7 ± 1.2*	
Ctrl	1.98 ± 0.08	-45.8 ± 2.0	5
AEA 500 nM	1.86 ± 0.11	-45.5 ± 2.1	
M1627K			
Ctrl	2.23 ± 0.15	-33.1 ± 1.9	6
CBZ 200 µm	1.94 ± 0.08*	-42.2 ± 1.9*	
Ctrl	2.01 ± 0.25	-35.9 + 2.5	6
RZ 30 µm	1.36 ± 0.13*	-65.1 ± 2.8*	
Ctrl	2.07 ± 0.22	-34.8 ± 1.3	5
RZ 3 µm	1.92 ± 0.18	-41.5 ± 2.2*	
Ctrl	2.22 ± 0.11	-31.8 ± 1.5	5
AEA 5 µM	1.81 ± 0.07*	-41.3 ± 1.7*	
Ctrl	2.28 ± 0.11	-32.9 ± 0.5	4
AEA 500 nM	2.18 ± 0.05	-33 ± 1.8	

[a]The decay time constant was measured using the transient current elicited at +20 mV and fit to a single-exponential. [b]The voltage dependence of steady-state fast inactivation was examined using a series of 200 ms conditioning pre-pulses from -120 mV to +30 mV, followed by a 20 ms test pulse to +15 mV to assess channel availability. The midpoint of activation was estimated by fitting the data with a Bolztmann function. *$p < 0.05$ from control by paired student's t-test.